Polarimetric Measurements of Sea Surface Brightness Temperatures Using an Aircraft K-Band Radiometer

Simon H. Yueh, William J. Wilson, *Senior Member, IEEE*, Fuk K. Li, *Senior Member, IEEE*, Son V. Nghiem, *Member, IEEE*, and William B. Ricketts

Abstract— **This paper presents the first experimental evidence that the polarimetric brightness temperatures of sea surfaces are sensitive to ocean wind direction in the incidenc eangle range of 30 to 50 degrees. Our experimental data were collected by a K-band (19.35 GHz) polarimetric wind radiometer (WINDRAD) mounted on the NASA DC-8 aircraft. A set of aircraft radiometer flights was successfully completed in November 1993. We performed circle flights over National Data Buoy Center (NDBC) moored buoys deployed off the northern California coast, which provided ocean wind measurements. The first WINDRAD flight was made on November 4, 1993. There was clear weather with a wind speed of 12 m/s at 330 degrees around the Pt. Arena buoy. We circled the buoy at three incidence angles, and all data when plotted as functions of azimuth angles show clear modulations of several Kelvin. At 40 degrees incidence angle, there is a 5 Kelvin peak-to-peak signal in the second Stokes parameter Q and the third Stokes parameter U. The Q data maximum is in the upwind direction and U has a 45 degrees phase shift in azimuth—as predicted by theory. There is also an up/downwind asymmetry of 2 Kelvin in the Q data, and 1 Kelvin in the U data. At 50 degrees incidence angle, the collected data show very similar wind direction signatures to the SSM/I model function. Additional flights were made on other days under cloudy conditions. Data taken at a wind speed of 8 m/s show that at 40 degrees incidence Q and U have a smaller azimuthal modulation of 3 Kelvin, probably due to the lower wind speed. Additionally, the simultaneously recorded video images of sea surfaces suggested that Q and U data were less sensitive to unpolarized geophysical variations, such as clouds and whitecaps, while the T_v and T_h increased by a few Kelvin when the radiometer beam crossed over clouds, or there was a sudden increase of whitecaps in the radiometer footprint. The results of our aircraft flights indicate that passive polarimetric radiometry has a strong potential for global ocean wind speed and direction measurements from space.**

I. Introduction

GLOBAL measurements of near surface ocean wind are crucial for many oceanographic and atmospheric studies. The near surface wind generates the momentum flux affecting ocean circulation and mixing and is the key driving force in air-sea interaction processes. A potential sensor for ocean wind remote sensing is the passive microwave radiometer. Examples of such radiometers include the Scanning Multichannel Microwave Radiometer (SMMR) flown on NIMBUS-7 and SEASAT and the Special Sensor Microwave/Imager (SSM/I) deployed on the Defense Meteorological Satellite Program (DMSP) missions [1]. Passive radiometers measure the thermal emission from sea surfaces, which is affected by surface roughness, temperature, foam, salinity, atmospheric water content and other factors. Although it is commonly accepted that microwave radiometers can measure ocean wind speeds based on the sensitivity of thermal emission on surface roughness, it was not clear whether passive microwave radiometer measurements were sensitive to wind direction until the recent experimental observations [2]-[4] indicated that ocean thermal radiation could vary over azimuthal angles relative to the wind by a few Kelvin.

Reference [2] measured the azimuthal dependence of brightness temperatures of vertical and horizontal polarizations (T_v and T_h) using their aircraft radiometers at near grazing (incidence angle of 78 degrees) at 20 GHz and at normal incidence at 3.7, 20, and 37 GHz. Their results showed that the azimuthal modulation dropped rapidly with increasing electromagnetic wavelength. Unfortunately, the measurements they reported did not include the range of incidence angle traditionally used by spaceborne microwave radiometers (incidence angles of about 48 degrees to 60 degrees) for large swath coverage.

In contrast, the SSM/I measures the brightness temperatures at an incidence angle of 53 degrees. Reference [3] colocated the SSM/I data with the buoy-measured wind vector and found that T_h and T_v at both 19 and 37 GHz could vary with the wind direction by a few Kelvin. Based on this wind direction signal, a monthly mean ocean wind map was produced from the SSM/I data [3], confirming the sensitivity of sea surface microwave radiations on ocean wind direction.

While conventional radiometers measure the brightness temperatures with vertical and horizontal polarizations, the results from [4] suggest that radiometric signatures at other polarization states are also sensitive to wind direction. In fact, the full polarization state of thermal emission from water surfaces can be characterized by four Stokes parameters I, Q, U, and V, which are related to the horizontal and vertical polarization components of the radiated electric fields illustrated in Fig. 1. Ground-based microwave radiometer measurements of water surfaces with artificially constructed directional features [5], [6] have shown that, in addition to I and Q, the third Stokes parameter U also had azimuthal variations. Nevertheless, although these ground-based studies provided valuable physical insight into the mechanisms responsible for the azimuth modulation signatures, the approximately sinusoidal surface profiles were too simplistic compared with sea surfaces.

Manuscript received February 7, 1994; revised August 24, 1994.

The authors are with the Jet Propulsion Laboratory, California Institute of Technology, Pasadena, CA 91109 USA.

IEEE Log Number 9407082.

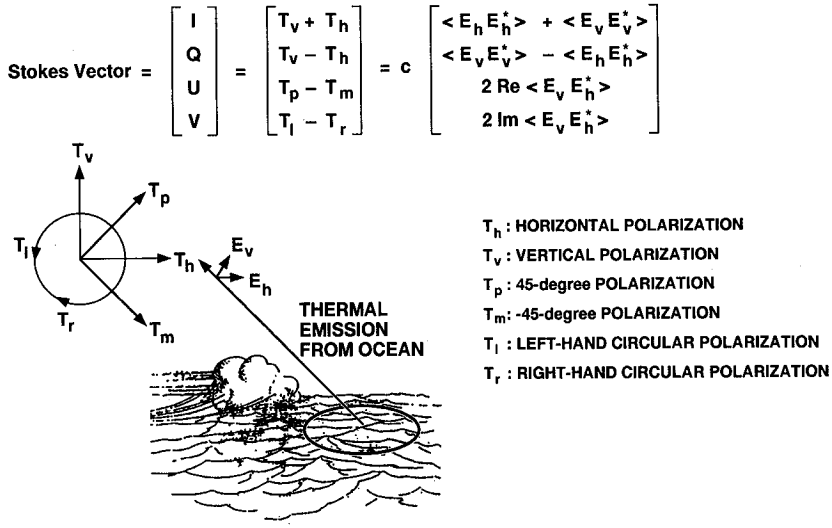

Fig. 1. Stokes parameters I, Q, U and V and their relations to the thermally radiated electric fields with two orthogonal components E_h and E_v. I signifies the total radiated power, while Q characterizes the polarization difference. The third parameter U and the fourth parameter V represent the real and imaginary parts of the mutual correlation between E_v and E_h. U (V) can be measured by taking the difference of T_p (T_r) and T_m (T_l), which are the brightness temperatures measured at 45 (Right-hand circular) and -45 degree linear (Left-hand circular) polarizations.

The experimental results presented in [4] were data collected by an aircraft Ku-band radiometer at normal incidence (incidence angle of 0 degree). Fig. 5 in their paper showed that when the second Stokes parameter reached maximum, the third Stokes parameter was nearly zero, and vice versa. The observed azimuthal variations of the second and third Stokes parameters have been shown to agree qualitatively with the predictions of a two-scale surface emission model analysis [8]. However, since only one example was reported and the data were collected at normal incidence, which is not so appropriate for space remote sensing if a large swath coverage is required, more extensive observations of the azimuthal variations of Stokes parameters over wind speeds and incidence angles are required to evaluate the applicability of polarimetric radiometry to ocean surface winds.

Theoretical studies of polarimetric emission in the middle range of incidence angles have been carried out by [8] using a two-scale sea surface model with the small scale surface scattering modelled by Bragg scattering [7]. Their results were in reasonable agreement with the data reported in [2] and the results of SSM/I data analysis in [3]. Additionally, it was found that the U parameter was an odd function with respect to the wind direction with its peaks occurring at approximately 45 degrees away from the wind direction, and its azimuth modulation magnitudes were comparable to that of Q parameter. Their study suggested that because of the relative azimuth phase shift between Q and U, it would be possible to achieve good wind vector measurements across all parts of swath using a spaceborne polarimetric radiometer. Although their theoretical results indicated promising applications, no experimental data collected in the incidence angle range of 30 to 60 degrees were yet available.

To explore the potential of the polarimetric radiometry technique for further space remote sensing consideration, a K-band multi-polarization radiometer was built and deployed on the NASA DC-8 aircraft with circle flights over several ocean buoys to study sea surface emissions. Section II describes the design of our K-band (19.35 GHz) microwave radiometer and our first set of aircraft experiments, and details the data reduction methods. The measured brightness temperature data are presented in Section III in terms of their correlation with wind direction. Section IV summarizes the results of this paper.

II. Multipolarization Microwave Radiometer Measurements and Data Calibration

To measure all four Stokes parameters, the WINDRAD, a K-band microwave multi-polarization wind radiometer, for ocean wind remote sensing was completed in October 1993. This radiometer is a direct detection Dicke-switch radiometer with noise injection to achieve better balance between alternating antenna and reference measurements. (The noise source was on when taking ocean measurements and off when the Dicke switch was switched to reference load.) All microwave components are mounted on a temperature-controlled plate to achieve good gain stability and are in a metallic box for thermal insulation and to prevent external microwave interference.

The radiometer block diagram is shown in Fig. 2 and its key parameters are shown in Table I. The electric fields entering the antenna are split into horizontal and vertical polarization components (E_h and E_v) by an orthogonal mode transducer (OMT). A microwave waveguide switch network depicted in Fig. 2 is then used to produce four polarizations using these two linearly polarized orthogonal components. In the waveguide switch network, a Magic-Tee is used to take the sum and the difference of vertically and horizontally polarized electric fields to produce the 45 and -45 degree linear polarizations with the phase shifter set at the 0-degree-phase position. If the phase shifter is set at the 90 degrees phase shift position by a manual switch, these two 45 and -45 linear polarizations become right- and left-hand circular polarizations. At each polarization setting, 22 pairs of antenna and reference load measurements were taken, corresponding to an integration time of 88 ms, and were reduced to one brightness temperature

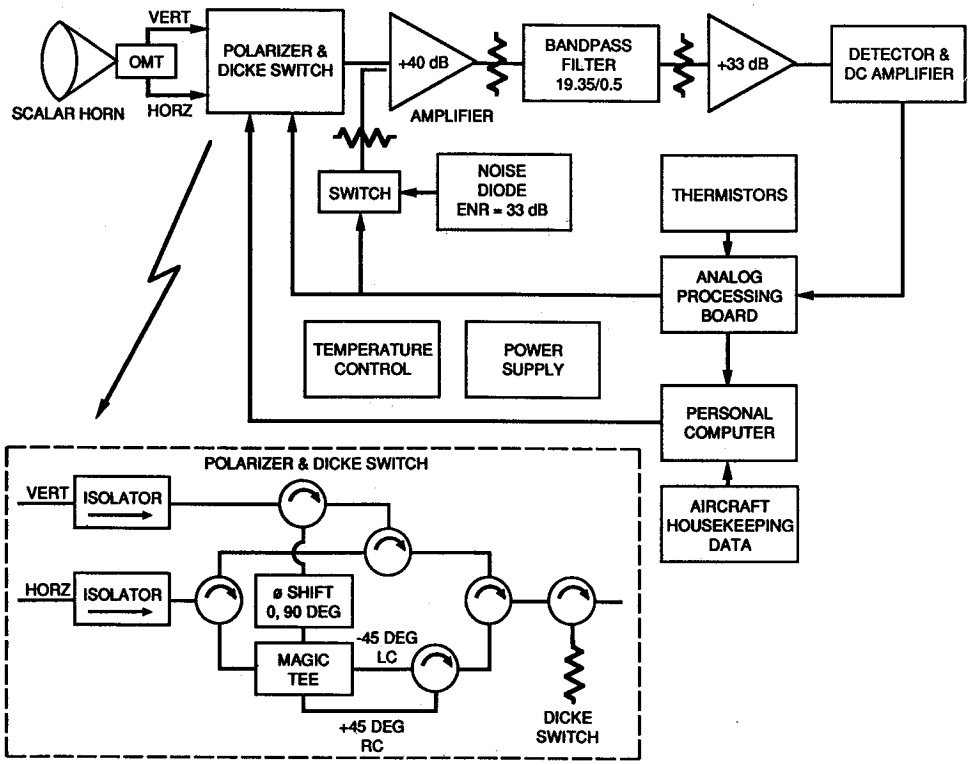

Fig. 2. WINDRAD block diagram.

TABLE I
WINDRAD KEY PARAMETERS

Parameter	Value
Frequency (GHz)	19.35
Antenna Beamwidth (degree)	3.6
Antenna Sidelobes (dB)	< -30
Polarization	V, H, 45(R*),-45(L*)
Dicke Switch Rate (Hz)	500
System Noise Temperature + Background (K)	530
Radiometer Bandwidth (MHz)	500

*: Phase shifter set at 90 degrees phase shift

sample. Four polarizations, including vertical, horizontal, −45 degree linear (left-hand circular), and 45 degree linear (right-hand circular) polarizations, were scanned sequentially with the switch positions commanded by a personal computer to obtain four brightness temperature samples, T_v, T_h, $T_m(T_l)$, and $T_p(T_r)$. Throughout our experiments, we did not use the 90-degree phase shift option because of limited available flight hours, and hence only the first three Stokes parameters were measured. To achieve a better radiometer sensitivity, we further average the data over 32 samples. This results in a radiometer sensitivity of 0.028 Kelvin for T_v and T_h data plotted in Figs. 4–6 and 8, and 0.04 Kelvin for Q and U data because Q and U were derived as the difference between two linear polarization measurements.

The radiometric calibration converting the radiometer voltage outputs into brightness temperatures was performed using the radiometer parameters measured in the laboratory and the ancillary thermistor measurements taken during the aircraft flights. To measure the noise diode temperature in the laboratory, we replaced the reference load by a small K-band horn (about 2 inches long), switched the Dicke switch to the small horn, and took the hot load (absorber) measurements with the noise diode switch on and off and the cold load (liquid nitrogen) measurements with the noise diode switch off. These measurements allowed us to calculate the noise diode temperature, which subsequently enabled us to calculate the losses for all polarization channels from the flight antenna to the Dicke switch using the hot/cold load calibration technique. During circle flights, the physical temperatures of the waveguide switch network, the reference load, the OMT, and the antenna horn were measured by using the thermistors attached on these components and recorded by the personal computer about once per minute allowing us to detect any sensible temperature changes. These losses and temperature measurements gave us the slope and the zero-intercept of the straight line for voltage to brightness temperature conversion. We examined the absolute accuracy of the conversion formula for each polarization channel by comparing the brightness temperatures of hot and cold loads against the temperature of the absorber measured by a thermistor and the liquid nitrogen temperature (77 Kelvin), and we found that the differences were less than 2 Kelvin for all polarization channels.

After its completion, the WINDRAD was mounted in the window of the NASA DC-8 aircraft. A set of radiometer flights over ocean surfaces were performed in November 1993 to measure polarimetric brightness temperatures of sea surfaces under a variety of wind/atmospheric conditions. We performed circle flights over selected NDBC moored buoys deployed off the coast of the northern California, which provided ocean wind speed and direction data in addition to other associated oceanic measurements. Because the antenna was fix-mounted on the DC-8 with an incidence angle of 60 degrees when the DC-8 flew level, the DC-8 was banked at several different roll angles to allow us to observe the ocean at various incidence angles.

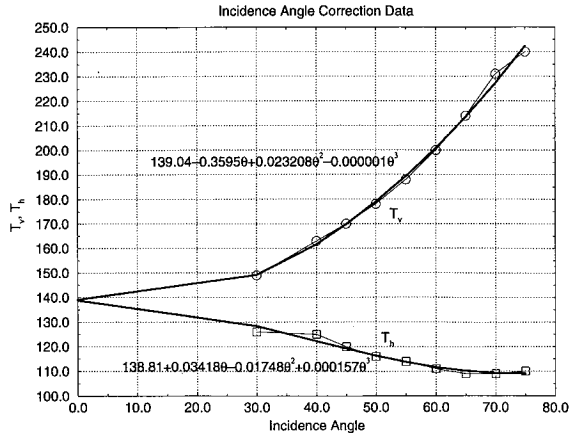

Fig. 3. Measured brightness temperatures as functions of incidence angle and third-order polynomial fits for incidence angle effect correction.

In addition to radiometer data and NDBC buoy data, aircraft navigation data transmitted through the DC-8 serial bus were also recorded by the personal computer. The DC-8 housekeeping data include the DC-8 pitch, roll and heading angles, ground speed, altitude, and etc. It was found that the DC-8 roll and pitch angles would typically change gradually by a few degrees during the circle flights. The main effect of the pitch angle drift is to cause an angular offest between the polarization basis vectors parallel to the antenna vertical and horizontal polarization channels and those with respect the water surface. However, with the knowledge of aircraft pitch and roll angles, we used the coordinate transformation between these two polarization coordinate systems to derive the relative alignment angle (χ) between these two sets of polarization vectors in addition to the incidence angle (θ) with respect to the water surfaces. Using the relative alignment angle, we then converted the Stokes parameters measured relative to the antenna coordinate into these with respect to the water surface coordinate using the following transformation:

$$I = I_a \tag{1}$$

$$Q = Q_a \cos 2\chi + U_a \sin 2\chi \tag{2}$$

$$U = U_a \cos 2\chi - Q_a \sin 2\chi \tag{3}$$

$$V = V_a \tag{4}$$

where the subscript 'a' indicates these quantities measured with respect to the antenna coordinate system, while quantities without subscript are defined in the water surface coordinate system.

Besides its effect on the polarization basis alignment, the aircraft attitude variation can also cause an incidence angle drift. The actual incidence angle was affected most significantly by the aircraft roll angle variation during circle flights. Because the incidence angle variations were expected to cause significant changes in the T_v and T_h brightness temperatures, we took additional brightness temperatures over a wide range of incidence angles from 30 to 80 degrees by wing-wagging the aircraft. Fig. 3 illustrates the measured brightness temperature data as a function of incidence angle and the corresponding third-order polynomial fits. Our approach for the incidence angle effect correction was to first calculate the average incidence angle over a full set of circles and then calculate the difference between the instantaneous incidence angle and the average angle. The difference is converted into an expected brightness temperatures variation using the empirical third-order polynomials, which is then used to translate the measured T_v and T_h data into those that would be measured as if the incidence angle had remained constant at the average incidence angle. After we inspected the T_v, T_h, and Q data measured with multiple continuous circles, the data after correction were nearly symmetric with respect to the wind direction and more repeatable over the sequence of circles, indicating that the above-mentioned empirical correction technique performed reasonably well. Although this empirical approach appeared reasonable, we recognize that it could only provide a first-order correction and some errors remain uncompensated, since brightness temperatures are expected to be functions of other environmental variables like cloud water and may not be correctly modelled by polynomials with fixed coefficients.

Note that similar incidence angle correction was not carried out for the U data, since U seemed to be a relatively weak function of incidence angle because the data collected from 30 to 50 degrees incidence showed that U apparently varied by less than 1 Kelvin over a change of 20 degrees incidence angle. Hence the incidence angle correction was not deemed necessary.

Our third Stokes parameter U data is in fact derived from the 45 and -45 degrees polarization brightness temperatures denoted by T_p and T_m (see Fig. 1). If there is cross-coupling between the antenna horizontal and vertical channels, or if the losses between these two polarization channels leading from the OMT to the Magic-Tee outputs are not perfectly compensated by calibration, or if the antenna mount is not aligned exactly with the DC-8 body coordinate axes, the resulting U measurements will have bias terms. This error term can be shown to have the following form, if a linear system is assumed for our radiometer:

$$\Delta U = c_1 T_v + c_2 T_h + c_3 \tag{5}$$

We estimated these three coefficients using the data itself based on the fact that the average value of U over a complete circle should be zero because U should be an odd function with respect to the wind direction [11]. For each set of circle flight, we averaged the values of U, T_v, and T_h over a complete circle. Using all circle flights data, we performed a linear-regression of the U-average data (not zero) with the T_v and T_h data. The resulting estimation was c_1 =0.0194, $c_2 = -0.00926$, and $c_3 = -2.634$, and the rms difference between the U-bias term estimated using the linear-regression curve and the measured U-average data was 0.22. The bias correction formula was used to correct the U data using the coincidental T_v and T_h measurements. We found that the DC-bias terms seen in the original U data were effectively removed, while there was no noticeable change in the shape of U data with respect to the azimuth angle.

III. Azimuth Signatures of Measured Stokes Parameters

To study the azimuthal modulations of brightness temperatures, we correlated the multi-polarization measurements with

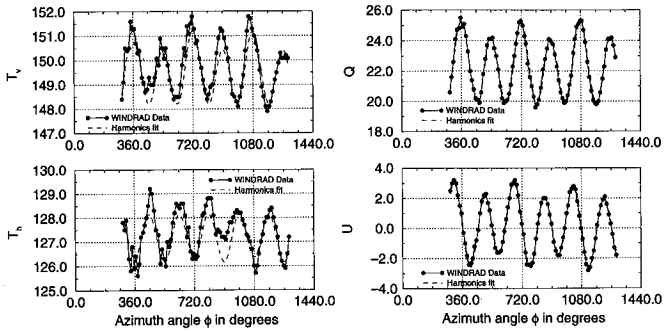

Fig. 4. Measured Stokes parameters at 30 degrees incidence versus azimuth angle indicated by solid curves. About two and half circles of data were plotted continuously in azimuth angle with incremental 360 degrees added to each additional circle flight. Because the flight circle center drifted in time, the radiometer footprint did not return to the same surface spot after a complete circle. The aircraft flight altitude was about 30 000 ft for the first circle, and after that the aircraft performed descending spiral to about 15 000 ft at the end of circle flight. Buoy closest to the circle reported 23 knots at 5 m elevation, which can be translated into 12 m/s at 20 m elevation based on [10]. Dashed curves represent the second harmonic approximation.

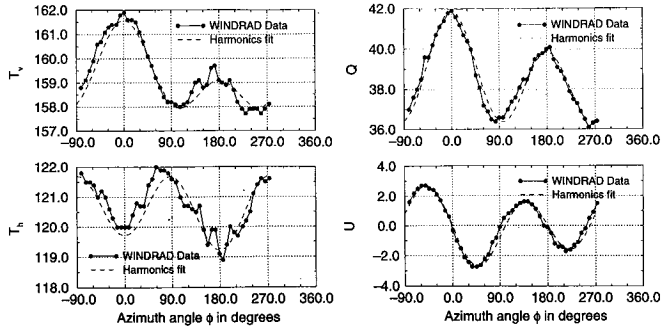

Fig. 5. Measured Stokes parameters at 40 degrees incidence versus azimuth angle indicated by solid curves. The aircraft flight altitude was about 27 000 ft. Buoy closest to the circle reported 23 knots at 5 m elevation, which can be translated into 12 m/s at 20 m elevation based on [10]. Dashed curves represent the second harmonic approximation.

the azimuth angle ϕ, the angle between the wind direction (ϕ_w) and the radiometer azimuth look angle (ϕ_r), i.e., $\phi = \phi_w - \phi_r$. With this definition, $\phi = 0$ (180) degrees corresponds to the upwind (downwind) direction. Because the NDBC buoys provide wind speed and direction measurements only once per hour, the buoy data collected at the time closest to the time of each circle flight is used. This is not expected to cause significant error because for our flights, we found that the buoy measured wind before and after the circle flights changed by less than or equal to 10 degrees in direction and less than 2 knots in speed. Hence, no interpolation was performed to estimate the wind speed and direction at the exact time of flight.

Fig. 4 illustrates the measured Stokes parameters, collected at 30 degrees incidence, as functions of azimuth angle ϕ. There are clear azimuth modulations in all measured Stokes parameters with an approximate 3 Kelvin peak-to-peak signal in T_v and T_h and a 5 Kelvin signal in Q and U data. The peaks of T_v occur at up/downwind direction, and the minima at crosswind direction, while T_h peaks at crosswind direction and reaches minimum at up/downwind direction. These modulation signatures agree with the data collected at normal incidence in [2], [4], the SSM/I model function [3], ground-based measurements [5], [6] and the theoretical predictions in [7], [8]. However, unlike the normal incidence measurements and the ground-based experiments using symmetric surfaces, there are up/downwind asymmetry (brightness difference between the up and downwind direction measurements) of about 1.3, 0.2, and 1.1 Kelvin in T_v, T_h, and Q, respectively, in our aircraft data. This up/downwind asymmetry could be caused by the hydrodynamic modulation of the capillary waves, or could be explained by the observations that the whitecaps in the downwind side are brighter than those in the upwind side [9]. In addition, it can be noticed that along the wind direction, U is close to (should be according to reflection symmetry) zero and reaches maximum at about 45 degrees away from the wind direction. Furthermore, unlike T_v, T_h, and Q data, U is an odd function of azimuth angle with respect to the wind direction. The relative azimuth phase shift between U and Q data may lead to good wind measurement performance across all parts of swath as discussed in [7].

Taking a closer look at Fig. 4, we noticed that T_v and T_h curves had a few spikes located at several azimuth angles, for example, 367, 636, 687, and 900 degrees, and were not as smooth as Q and U data. In particular, the noise near $\phi = 900$ degrees significantly smoothed out the expected T_h minimum along the downwind direction. However, these additional signals were apparently unpolarized, and hence, did not introduce corresponding effects in the Q and U data. After we visually reviewed the video tape recorded at the same time with the brightness measurements, it appeared that at these few moments, there were isolated, sudden increases of wave breakings and sustained whitecaps in the radiometer footprint. Therefore it would not be surprising to find simultaneous brightness temperature increases of 1 to 2 Kelvin in all radiometer channels [9]. Another potential cause for these "noises" is the wind gust, which could roughen the surface, create significant wide-spread whitecaps, and result in a simultaneous increase of signal in all polarization channels. However, due to the lack of coincidental surface ground truth measurements, the exact cause of these noises remains to be investigated. In any case, the fact that Q and U are insensitive to these noises suggests that Q and U are less susceptible to unpolarized geophysical variations.

Fig. 5 plots the data collected at 40 degrees incidence angle. The azimuth signatures of all measured Stokes parameters as well as the peak-to-peak signals are similar to those taken at 30 degrees incidence, indicating that the wind direction signals are smooth function of incidence angle from 30 to 40 degrees. Again the spikes in the T_v and T_h data around the azimuth angle of 180 degrees are found at times with enhanced breaking waves and whitecaps.

Besides the data mentioned above, one circle flight was also performed for the incidence angle of about 50 degrees with an average value of 49 degrees, and the Stokes parameter data are illustrated in Fig. 6. To allow easy comparison with the SSM/I wind direction signal, the model function reduced from the SSM/I data by Wentz [3] at the measured wind speed are also included. To place the SSM/I data together with our data, we added constant offsets of 4 and 25.5 to the SSM/I T_v and T_h model, respectively, which were

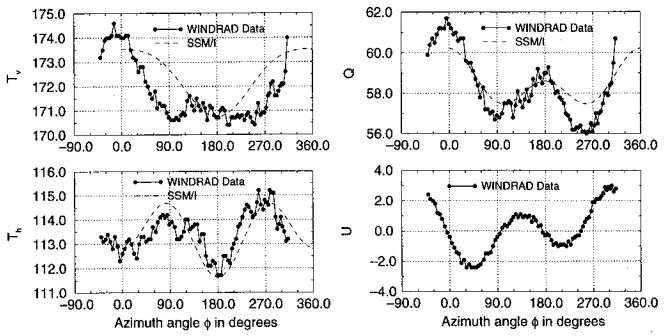

Fig. 6. Measured Stokes parameters at 50 degrees incidence versus azimuth angle indicated by solid curves. The aircraft flight altitude was about 27 000 ft. Buoy closest to the circle reported 23 knots at 5 m elevation, which can be translated into 12 m/s at 20 m elevation based on [10]. Dashed curve represents the SSM/I model function.

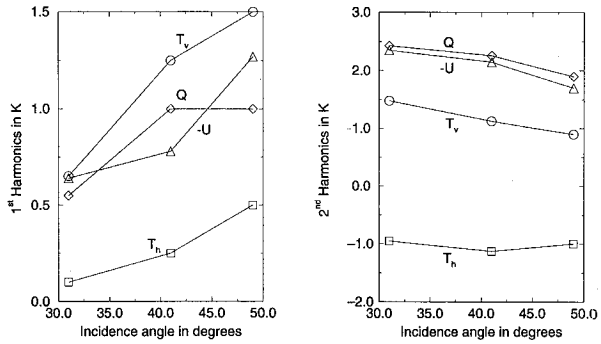

Fig. 7. Harmonic coefficients of Stokes parameters plotted as functions of incidence angle. Buoy closest to the circle reported 23 knots at 5 m elevation, which can be translated into 12 m/s at 20 m elevation based on [10].

possibly due to the atmospheric radiation and the difference in incidence angles (49 degrees for our data against 53 degrees for the SSM/I). In Wentz's SSM/I model function, the contribution of atmospheric radiation has been estimated and removed using the 22 and 37 GHz channels, while since our system had only one frequency channel, it was not possible to remove the atmospheric effects from our measurements. Note that there is a significant difference between these two offsets, which could be due to that the sea surfaces are better reflectors for horizontal polarization than vertical polarization, hence, reflecting more horizontally polarized downwelling atmospheric radiation than vertically polarized radiation into the receiver, and could also be caused by the incidence angle difference of 4 degrees, resulting in different sea surface emissivities at these two incidence angles with an expected enhancement in T_h offset, while a reduction in T_v offset according to the incidence angle effects illustrated in Fig. 3. Nevertheless, the azimuth modulation signatures of our T_v and T_h data show a close resemblance to the SSM/I data collected at 53 degrees incidence, and in particular the vertical polarization brightness T_v, like the SSM/I model, did not have an obvious peak in the downwind direction. The absence of brightness peak in the downwind direction in the T_v data results in the observed, relatively small second harmonic coefficient.

A typical form of geophysical model functions, relating the thermal radiation signatures to the geophysical surface parameters, expresses the Stokes parameters in the Fourier series of the azimuth angle ϕ. For wind-generated sea surfaces, it is expected that the surfaces are statistically reflection symmetric with respect to the wind direction represented by $\phi = 0$. Using reflection symmetry and Maxwell's equations, [11] has shown that I and Q (or T_v and T_h) are even functions of ϕ, whereas U and V are odd functions. Hence, expanded only to the second harmonic of ϕ

$$I \simeq I_0 + I_1 \cos\phi + I_2 \cos 2\phi \tag{6}$$

$$Q \simeq Q_0 + Q_1 \cos\phi + Q_2 \cos 2\phi \tag{7}$$

$$U \simeq U_1 \sin\phi = U_2 \sin 2\phi \tag{8}$$

$$V \simeq V_1 \sin\phi + V_2 \sin 2\phi. \tag{9}$$

Like I and Q, T_v and T_h are expanded by the cosine series.

We extracted the harmonic coefficients from the data presented in Figs. 4–6 and included the second harmonic approximation curves in Figs. 4 and 5 for comparison. We found that the second harmonic expansion appeared to be a good approximation, in particular for the Q and U parameters.

Fig. 7 illustrates the incidence angle dependence of the harmonic coefficients. The first harmonic coefficients of all Stokes parameters have a rising trend with increasing incidence angles, meaning that the up/downwind asymmetry is larger at a higher incidence angle. The first harmonic of T_v is about 3 times of that of T_h, indicating that vertical polarization is more strongly affected by the up/downwind asymmetric features of sea surfaces than horizontal polarization. Unlike the first harmonics, all the second harmonics have a slow decreasing trend as the incidence angle increases. The second harmonic modulation amplitudes of Q and U are about 2 times of that of T_v or T_h. That is, even though the radiometer signal sensitivity of Q and U, which are calculated as the difference between two polarization measurements, is typically $\sqrt{2}$ times of that of T_v or T_h, their increased sensitivity to wind direction will more than offset the lower SNR. It is interesting to notice that the harmonic coefficients of Q are close to that of U, consistent with the theoretical predictions in [7], [8]. It should be noted that the harmonic coefficients presented in this plot were derived from a very limited data set. However, the values of harmonic coefficients should represent very well the oceanic/atmospheric conditions encountered at the time of experiment because our radiometer sensitivity, being much smaller than the magnitudes of harmonic coefficients, should allow an interpretation of the trend of harmonic coefficients over incidence angles. Nevertheless, more experimental data are necessary to find the sensitivity of the harmonic coefficients on oceanic/atmospheric conditions.

The effects of clouds on the brightness temperature measurements are illustrated in Fig. 8. The data were taken at the incidence angle of about 40 degrees similar to the data plotted in Fig. 5, and at the time of flight, right after a cold front passed over the buoy off the northern California coast, there were many clouds scattered in the sky, and once a while there would be a piece of clouds lying between the sea surfaces and the antenna. It was found that while the radiometer beam crossed the clouds, as expected, the brightness temperatures in all polarization channels would increase simultaneously by

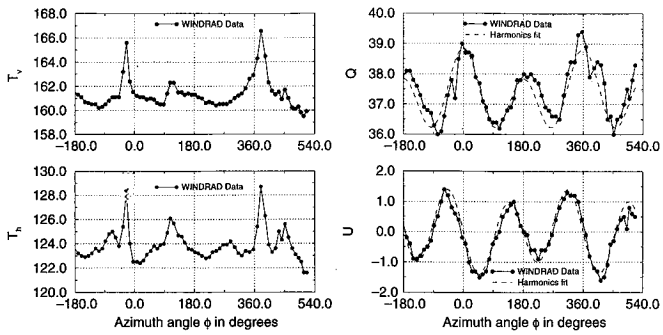

Fig. 8. Measured Stokes parameters at 40 degrees incidence versus azimuth angle indicated by solid curves. The aircraft flight altitude was about 16 000 ft. The sky was partially cloudy with scattered puffy clouds. Buoy closest to the circle reported 14 knots at 5 m elevation, which can be translated into 8 m/s at 20 m elevation based on [10]. Dashed curves represent the second harmonic approximation.

a few Kelvin, overwhelming the wind direction signals in T_v and T_h. In contrast, the Q and U data, which are expected to be insensitive to unpolarized radiations, are less affected by the clouds, displaying very similar azimuth signatures to the data taken under clear sky conditions shown in Figs. 4 to 6. This indicates that polarimetric brightness measurements are useful even under cloudy conditions.

Again comparing Fig. 5 with Fig. 8 shows that the peak-to-peak signals in the Q and U data in Fig. 5 are about 3 Kelvin, less than the 5 Kelvin signal shown in Fig. 5. This is probably related to the reduction of wind speed, about 8 m/s for the data presented in Fig. 8 compared with 12 m/s for Fig. 5.

IV. Summary

We have completed a set of proof-of-concept aircraft measurements of the K-band multi-polarization brightness temperatures of sea surfaces, detecting a few Kelvin dependence on wind direction. The WINDRAD data show that T_v, T_h and Q are even functions of the wind direction, while the third Stokes parameter U is an odd function—as predicted by a two-scale surface scattering model [8] and proved exactly by using Maxwell's equations along with a reflection symmetry assumption for wind-driven sea surfaces [11]. In addition, the data collected at 50 degrees incidence angle are very similar to the SSM/I brightness temperature data, particularly, the absence of vertical polarization peak in the downwind direction in both data sets. Comparing Q and U data curves with T_v and T_h curves indicates that Q and U data could be less sensitive to clouds, breaking waves and whitecaps, which are strong thermal radiation sources. This suggests that Q and U are potentially better indicators for wind direction measurements. In conclusion, our aircraft radiometer flights show that the first three Stokes parameters of the thermal radiation from sea surfaces have a sinusoidal variation relative to the wind direction from 30 to 50 degrees incidence with an amplitude of a few Kelvin.

We recognize that because of limited flight hours and the oceanic/atmospheric conditions encountered, it is not possible to develop a comprehensive geophysical model function using our existing data set to examine more quantitatively the sensitivities on wind speeds, incidence angles and other atmospheric and ocean variables. Hence, more extensive aircraft measurements are being performed to further our understanding of the multi-polarization brightness temperature signatures of sea surfaces.

Acknowledgment

This work was performed under contract with the National Aeronautics and Space Administration at the Jet Propulsion Laboratory, California Institute of Technology. The authors would like to thank R. Fenstermacker and D. Huynh for the development of radiometer control software and the NASA Ames Research Center for assistance in aircraft flight experiments.

References

[1] J. P. Hollinger, J. L. Peirce, and G. A. Poe, "SSM/I instrument evaluation," *IEEE Trans. Geosci. Remote Sensing*, vol. 28, pp. 781-790, Sept. 1990.

[2] V. S. Etkin, M. D. Raev, M. G. Bulatov, Y. A. Militsky, A. V. Smirnov, *et al. Radiohydrophysical Aerospace Research of Ocean*, Report Пр-1749, Academy of Sciences, Space Research Institute, Moscow, USSR, 1991.

[3] F. J. Wentz, "Measurement of oceanic wind vector using satellite microwave radiometers," *IEEE Trans. Geosci. Remote Sensing*, vol. 30, pp. 960-972, Sept. 1992.

[4] M. S. Dzura V. S. Etkin, A. S. Khrupin, M. N. Pospelov, and M. D. Raev, "Radiometers-polarimeters: principles of design and applications for sea surface microwave emission polarimetry," *Int. Geosci. Remote Sensing Symp.*, Houston, TX, 1992.

[5] J. T. Johnson, J. A. Kong, R. T. Shin, D. H. Staelin, K. O'Neill, and A. W. Lohanick, "Third Stokes parameter emission from a periodic water surface," *IEEE Trans. Geosci. Remote Sensing*, vol. 31, pp. 1066-1080, Sept. 1993.

[6] S. H. Yueh, S. V. Nghiem, R. Kwok, W. J. Wilson, F. K. Li, *et al.*, "Polarimetric thermal emission from periodic water surfaces," *Radio Sci.*, Jan./Feb., 1994.

[7] ——, "Polarimetric passive remote sensing of ocean wind vector," *Radio Sci.*, July/Aug., 1994.

[8] ——, "Polarimetric passive remote sensing of wind-generated sea surfaces and ocean wind vectors," *Proc. Ocean Symp.*, vol. 1, Victoria, BC, Canada, Oct. 1993, pp. 31-36.

[9] P. M. Smith, "The emissivity of sea foam at 19 and 37 GHz," *IEEE Trans. Geosci. Remote Sensing*, vol. GE-26, 541-547, 1988.

[10] W. J. Pierson, "The theory and applications of ocean wave measuring systems at and below the sea surface, on the land, from aircraft, and from spacecraft," NASA Contract Rep. CR-2646, N76-17775, 1976.

[11] S. H. Yueh, R. Kwok, and S. V. Nghiem, "Polarimetric scattering and emission properties of targets with reflection symmetry," *Radio Sci.*, in press.

Simon H. Yueh received the S.B. and S.M. degrees from National Taiwan University, Taiwan, and the Ph.D. degree in electrical engineering from the Massachusetts Institute of Technology, Cambridge, in 1982, 1984, and 1991, respectively.

He was a Postdoctoral Research Associate at the Massachusetts Institute of Technology from February to August 1991. He developed various techniques for the calibration of polarimetric radars and theoretical models for the remote sensing of rough surfaces and random media. In 1991, he joined the SAR Systems Development and Processing Group at the Jet Propulsion Laboratory, Pasadena, CA, where he is Sensor Verification Team Leader for post-launch calibration of NASA Scatterometer. He has developed airborne polarimetric radiometers for ocean remote sensing and conducted experiments demonstrating the sensitivity of polarimetric brightness temperatures to ocean surface wind vectors. His current fields of interest include techniques and instrument developments for microwave remote sensing of ocean winds and polar ice, theories for active and passive microwave remote sensing, and applications of interferometric and polarimetric SAR data.

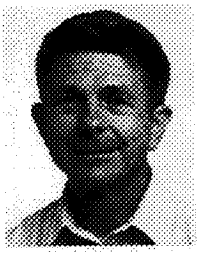

William J. Wilson (S'59–M'64–SM'80) received the B.S.E.E. degree from the University of Seattle, and the M.S.E.E., E.E., and Ph.D. degrees in electrical engineering from the Massachusetts Institute of Technology, Cambridge, in 1961, 1963, 1964, and 1970, respectively.

In 1964, he served in the U.S. Air Force, working on military communication satellites. In 1970, he joined the Aerospace Corporation, Los Angeles, CA, and was involved in the design and construction of millimeter-wave receivers and radio astronomy observations. In 1976–1977, he was an Assistant Professor in the Electrical Engineering Department, University of Texas, Austin. He returned to Aerospace in 1977, where he was involved with research in millimeter-wave radiometers and low-noise receivers. In 1980, he joined the staff of NASA's Jet Propulsion Laboratory, Pasadena, CA, and is the Supervisor of the Microwave Advanced Systems Group, where he has been working on low-noise millimeterwave radiometers and radar systems for aircraft and spacecraft for Earth remote sensing applications. He is currently a Senior Research Engineer. He has published more than 100 technical papers and reports.

Fuk K. Li (SM'89) was born in Hong Kong, in 1953. He received the B.Sc. and Ph.D. degrees in physics from the Massachusetts Institute of Technology, Cambridge, in 1975 and 1979, respectively.

He joined the Jet Propulsion Laboratory, California Institute of Technology, Pasadena, in 1979 where he has been involved in various radar remote sensing activities. He has developed a number of system analysis tools for spaceborne synthetic aperture radar (SAR) system design, a digital SAR processor and simulator for the analysis of SEASAT SAR data, investigated techniques for multi-look processing and Doppler parameter estimations for spaceborne SAR's and evaluated the tradeoffs in SAR image parameters. He also participated in the development of system design concepts and applications for interferometric SAR. From 1983 to 1988, he was the supervisor of a group involved in system design and engineering for spaceborne radars, airborne scatterometer experiment for ocean wind remote sensing, multipolarization SAR analysis technique development and electromagnetic scattering research. He was the Project Engineer for the NASA Scatterometer and was responsible for the technical design of the system. He conducted experiments that demonstrated the importance of wind stress in ocean backscatter. He was also responsible for the design of several advanced radar systems, including a synthetic aperture scanning altimeter, a spaceborne rain mapping radar, and a Titan radar mapper.

He is at present a principal investigator in airborne scatterometry experiments that will be conducted to refine the geophysical model function relating radar backscatter to ocean winds. He is also the principal investigator for an airborne rain mapping radar that will be flown to support the algorithm development and performance verification of the rain radar on the Tropical Rainfall Measurement Mission. He is the principal investigator for an experiment utilizing the SIR-C and XSAR systems to study rainfall effects on ocean roughness, mean Doppler motion of rain drips and rain retrieval with L-,.C-, and X-band observations from space. He is currently the Manager of the Radar Science and Engineering section.

Dr. Li was awarded the IEEE Aerospace and Electronic System Society 1990 Radar Systems Panel Award.

S. V. Nghiem (M'94) received the B.S. in electrical engineering from Texas A&M University, College Station, and the M.S. and Ph.D. degrees from the Massachusetts Institute of Technology, Cambridge, in 1985, 1988, and 1991, respectively.

Since 1991, he has joined the SAR Systems Development and Engineering Group, Radar Science and Engineering Section, Jet Propulsion Laboratory, California Institute of Technology, Pasadena. His work encompasses electromagnetic wave theory, model development for geophysical media, and polarimetric active and passive remote sensing.

Dr. Nghiem is a member of Phi Kappa Phi and Sigma Xi.

William B. Ricketts was born February 5, 1929, in Los Angeles, CA. He is a graduate of the U.S. Air Force Electronics and Advanced Radar School, Biloxi, MS.

From 1952 to 1958, he served as Senior Microwave Field Engineer for Gilfillan Bros., and was responsible for the installation and operation of ground controlled approach radar stations in the United States and Europe. He was employed from 1958 to 1960, as a Research Assistant in the Falcon Missile Receiver Group at Hughes Aircraft. In 1960, he joined Aerojet Electrosystem Co., as a Senior Engineer in the Microwave Systems Department and participated in the design and development of numerous airborne microwave radiometers. Since 1975, he has been with the Jet Propulsion Laboratory, Pasadena, CA, where he has been involved with the design and development of millimeter and submillimeter-wave radiometer systems.